Multiobjective Evolutionary Computation for Supersonic Wing-Shape Optimization

Shigeru Obayashi, Daisuke Sasaki, Yukihiro Takeguchi, and Naoki Hirose

***Abstract*—This paper discusses the design optimization of a wing for supersonic transport (SST) using a multiple-objective genetic algorithm (MOGA). Three objective functions are used to minimize the drag for supersonic cruise, the drag for transonic cruise, and the bending moment at the wing root for supersonic cruise. The wing shape is defined by 66 design variables. A Euler flow code is used to evaluate supersonic performance, and a potential flow code is used to evaluate transonic performance. To reduce the total computational time, flow calculations are parallelized on an NEC SX-4 computer using 32 processing elements. The detailed analysis of the resulting Pareto front suggests a renewed interest in the arrow wing planform for the supersonic wing.**

***Index Terms*—Aerodynamics, aircraft, genetic algorithms, optimization methods.**

I. Introduction

THE development of next-generation supersonic transport is being considered worldwide to respond to the increasing demand on air traffic. The aerodynamic design of such aircraft must account for drag reduction as well as sonic boom minimization. However, drag reduction is in conflict with sonic boom minimization. Since the acceptability of supersonic transport is very sensitive to sonic booms over populated areas, one of the design choices is to allow supersonic flight over sea, and to only have transonic flight over land. Although such a decision excludes the sonic boom from the design consideration, the design is now faced with transonic performance of the aircraft.

This paper considers the multipoint aerodynamic optimization of a wing shape for supersonic aircraft, both at a supersonic cruise condition and at a transonic cruise condition. Aerodynamic drag will be minimized at both cruise conditions under lift constraints. The aerodynamic optimization of the wing planform, however, drives the wing to have an impracticably large aspect ratio. In reality, the aspect ratio of the wing is constrained by other disciplines, such as structure and equipment.

In standard aircraft design procedure, the wing planform shape has to be determined at an early stage because the planform shape is closely related to aircraft sizing. In this stage, designers should account for tradeoffs among aerodynamic performance, structural strength and weight, fuel storage, and so on. Therefore, an automated design of the wing planform shape requires multidisciplinary design optimization (MDO) based on a system composed of aerodynamics, structural dynamics, etc. [1]. Because cross-disciplinary tradeoffs are built into the MDO model implicitly, a highly sophisticated MDO model is needed to obtain realistic wing planform shapes.

For the simplicity of the present wing model, however, the MDO model of a wing is not considered. Instead, the aerodynamic load is minimized by assuming that less aerodynamic load will lead to a lighter, sustaining wing structure. Therefore, minimization of the wing root bending moment is added as a third design objective. On the other hand, the present wing model does not have any built-in cross-disciplinary tradeoffs originally because no wing structure is specified. This means that each design objective may be treated independently.

The present optimization problem can be regarded as multiobjective (MO) optimization. MO optimization seeks to optimize the components of a vector-valued objective function. Unlike single-objective optimization, the solution to this problem is not a single point, but a family of points known as the Pareto-optimal set. Thus, it is more natural to find a set of compromise solutions, known as Pareto solutions, than to find a single optimal solution corresponding to a particular tradeoff.

By maintaining a population of solutions, genetic algorithms (GA) (or other evolutionary algorithms) can search for many Pareto-optimal solutions in parallel. This characteristic makes GA's very attractive for solving MO problems. As a solver for MO problems, the following two features are desired: 1) the solutions obtained are Pareto optimal, and 2) they are uniformly sampled from the Pareto-optimal set. To achieve these, MOGA's have been introduced successfully in [2].

Furthermore, it was shown that the so-called best N selection helps to find the extreme Pareto solutions [3]. This form of selection picks up the best N individuals among N parents and N children for the next generation in a manner similar to CHC [4]. The extreme Pareto solutions are the optimal solutions of the single objectives. By examining the extreme Pareto solutions, the quality of Pareto solutions can be measured. The present MO problem will be solved by using MOGA coupled with the best N selection.

II. Approach

In GA's, the natural parameter set of the optimization problem is coded as a finite-length string. Traditionally, GA's use binary numbers to represent such strings: a string has a finite length, and each bit of a string can be either 0 or 1. For real-valued function optimization, however, it is more natural to use real

Manuscript received June 28, 1999; revised November 15, 1999. This work was supported by the Japanese Government's Grants-in-Aid for Scientific Research under Grant 10305071. The work of S. Obayashi was supported in part by Bombardier Aerospace, Toronto, Ont., Canada.

S. Obayashi, D. Sasaki, and Y. Takeguchi are with the Department of Aeronautics and Space Engineering, Tohoku University, Sendai 980-8579, Japan (e-mail: obayashi@ieee.org).

N. Hirose is with the Computational Science Division, National Aerospace Laboratory, Tokyo 182-8522, Japan.

Publisher Item Identifier S 1089-778X(00)04475-1.

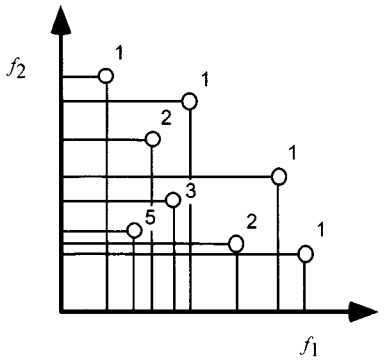

Fig. 1. Pareto ranking method for maximization of f_1 and f_2.

numbers (as might be done with evolution strategies or evolutionary programming). The length of the real-number string corresponds to the number of design variables.

A. Crossover and Mutation

A simple crossover operator for real-valued strings is the average crossover [5], which computes the arithmetic average of two real numbers provided by the mated pair. In this paper, a weighted average is used as

$$\begin{aligned}\text{Child1} &= ran1 \cdot \text{Parent1} + (1 - ran1) \cdot \text{Parent2} \\ \text{Child2} &= (1 - ran1) \cdot \text{Parent1} + ran1 \cdot \text{Parent2}\end{aligned} \tag{1}$$

where Child1, 2 and Parent1, 2 denote encoded design variables of the children (members of the new population) and parents (a mated pair of the old generation), respectively. The uniform random number $ran1$ in [0, 1] is regenerated for every design variable.

Mutation takes place at a probability of 0.2 initially, and the rate declines linearly during the evolution. Equation (1) will then be replaced by

$$\begin{aligned}\text{Child1} &= ran1 \cdot \text{Parent1} + (1 - ran1) \cdot \text{Parent2} \\ &\quad + m \cdot (ran2 - 0.5) \\ \text{Child2} &= (1 - ran1) \cdot \text{Parent1} + ran1 \cdot \text{Parent2} \\ &\quad + m \cdot (ran2 - 0.5)\end{aligned} \tag{2}$$

where $ran2$ is also uniform random numbers in [0, 1] and m determines the range of possible mutation.

B. Multiobjective Pareto Ranking

To search Pareto-optimal solutions by using MOGA, the ranking selection method [6] can be extended to identify the near-Pareto-optimal set within the population of GA. To do this, the following definitions are used: suppose $\boldsymbol{x}_i$ and $\boldsymbol{x}_j$ are in the current population, and $\boldsymbol{f} = (f_1, f_2, \cdots, f_q)$ is the set of objective functions to be maximized.

1) $\boldsymbol{x}_i$ is said to be dominated by (or inferior to) $\boldsymbol{x}_j$ if $\boldsymbol{f}(\boldsymbol{x}_i)$ is partially less than $\boldsymbol{f}(\boldsymbol{x}_j)$, i.e., $f_1(\boldsymbol{x}_i) \le f_1(\boldsymbol{x}_j) \wedge f_2(\boldsymbol{x}_i) \le f_2(\boldsymbol{x}_j) \wedge \cdots \wedge f_q(\boldsymbol{x}_i) \le f_q(\boldsymbol{x}_j)$ and $\boldsymbol{f}(\boldsymbol{x}_i) \ne \boldsymbol{f}(\boldsymbol{x}_j)$.
2) $\boldsymbol{x}_i$ is said to be nondominated if there does not exist any $\boldsymbol{x}_j$ in the population that dominates $\boldsymbol{x}_i$

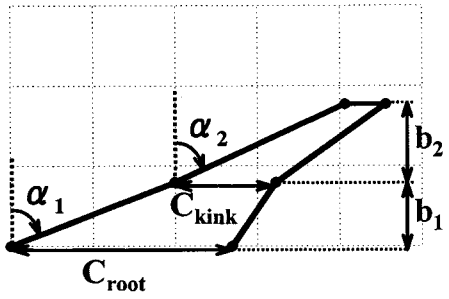

Fig. 2. Wing planform definition based on six design variables.

TABLE I
DOMAIN FOR WING PLANFORM DESIGN VARIABLES

Variable	Range
α_1	35 - 70 deg
α_2	35 - 70 deg
C_{root}	10 - 20
C_{kink}	3 - 5
b_1	2 - 7
b_2	2 -7

Nondominated solutions within the feasible region in the objective function space give the Pareto-optimal set.

Let us consider the following optimization:

$$\begin{aligned}&\text{maximize:} \quad f_1 = x, \quad f_2 = y \\ &\text{subject to:} \quad x^2 + y^2 \le 1 \quad \text{and} \quad 0 \le x, y \le 1.\end{aligned}$$

The Pareto front of the present test case becomes a quarter arc of the circle $x^2 + y^2 = 1$ at $0 \le x, y \le 1$.

Consider an individual $\boldsymbol{x}_i$ at generation t (Fig. 1) which is dominated by p_i^t individuals in the current population. Following [2], its current position in the individuals' rank can be given by

$$\text{rank}(\boldsymbol{x}_i, t) = 1 + p_i^t. \tag{3}$$

All nondominated individuals are assigned rank 1, as shown in Fig. 1. The fitness values are reassigned according to rank as an inverse of their rank values. Then the stochastic universal sampling (SUS) method [7] takes over with the reassigned values.

C. Fitness Sharing

To sample Pareto-optimal solutions from the Pareto-optimal set uniformly, it is important to maintain genetic diversity. The model used here to accomplish this is called fitness sharing (FS) [6]. The sharing function depends on the distance between individuals, which can be measured with respect to a metric in either genotypic or phenotypic space. A genotypic sharing measures the interchromosomal Hamming distance. A phenotypic sharing can further be classified into two types. One measures the distance between the decoded design variables. The other, in constrast, measures the distance between the designs' objective function values. Here, the latter phenotypic sharing is employed since we seek a global tradeoff surface in the objective function space.

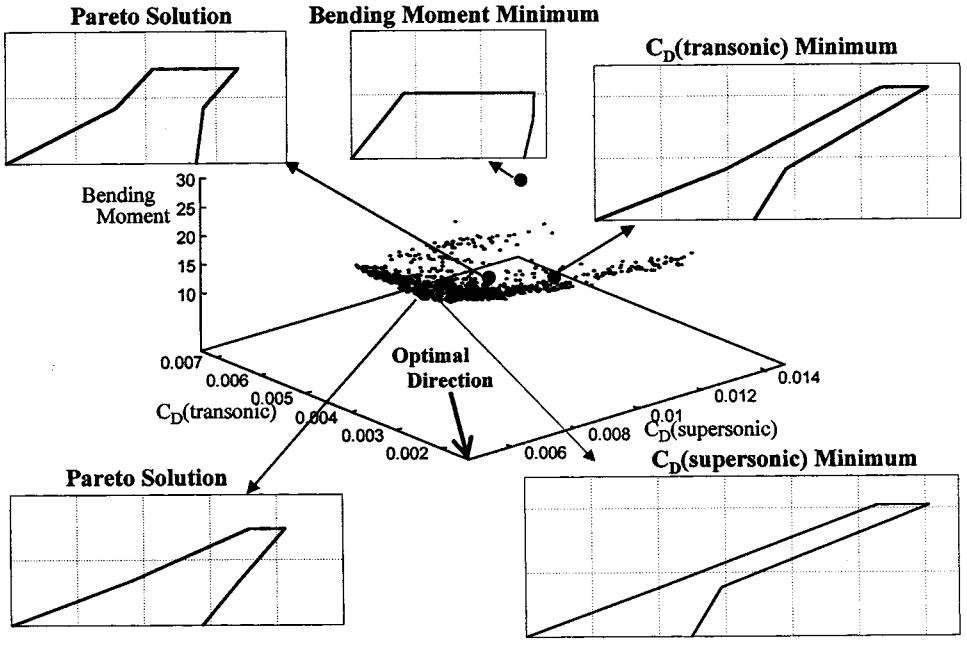

Fig. 3. Pareto solutions in the objective function space defined by supersonic and transonic drag coefficients and bending moment along with the sample wing planform shapes.

This scheme introduces a new parameter, the niche size σ_{share}. The choice of σ_{share} has a significant impact on the performance of MOGA's. Reference [2] gave a simple estimation of σ_{share} in the objective function space as

$$N\sigma_{\text{share}}^{q-1} - \frac{\prod_{i=1}^{q}(M_i - m_i + \sigma_{\text{share}}) - \prod_{i=1}^{q}(M_i - m_i)}{\sigma_{\text{share}}} = 0 \tag{4}$$

where N is a population size, q is a dimension of the objective vector, and M_i and m_i are maximum and minimum values of each objective, respectively. This formula has been adapted successfully here. Since this formula is applied at every generation, the resulting σ_{share} is adaptive to the population during the evolution process. Niche counts can be consistently incorporated into the fitness assignment according to rank by using them to scale individual fitness within each rank.

D. Physical Model

Aerodynamic forces acting on aircraft can be obtained from integrating the pressure and friction of air on the aircraft surface. The pressure and friction can be calculated by solving the governing equations of fluid. The fluid model determines the complexity of physics considered. For the aircraft design, the potential flow is often assumed. This fluid model is used for the transonic flow in this study. For the supersonic flow, a more complicated fluid model is used here to allow more shape variations of wing planforms. Such fluid is governed by the Euler equations.

The present optimization problem can be stated as follows.

Objective Functions:

1) Supersonic drag coefficient $C_{D,s}$.

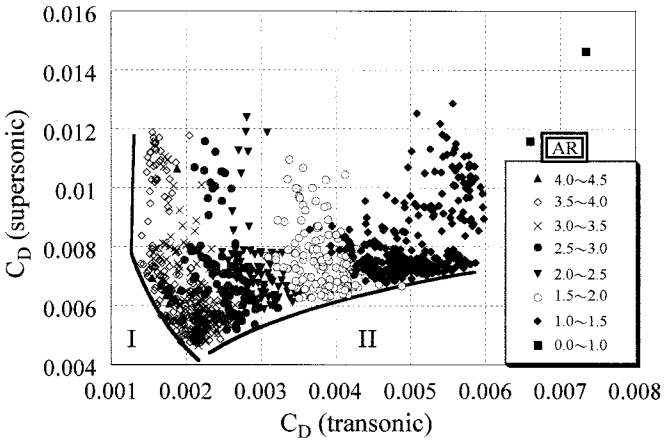

Fig. 4. Tradeoffs between supersonic and transonic drag coefficients represented by the projection of Pareto solution.

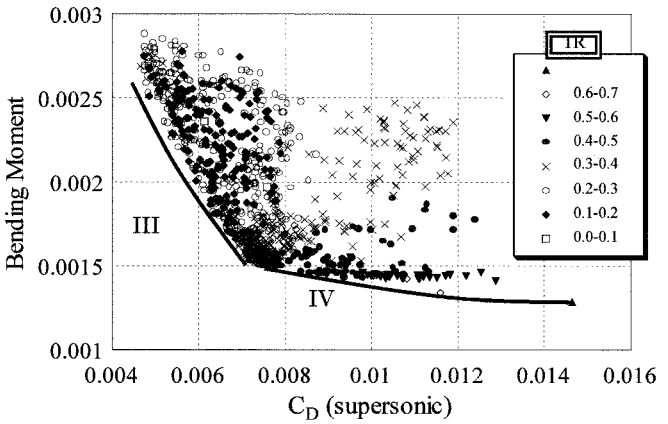

Fig. 5. Tradeoffs between bending moment and supersonic drag coefficients represented by the projection of Pareto solutions.

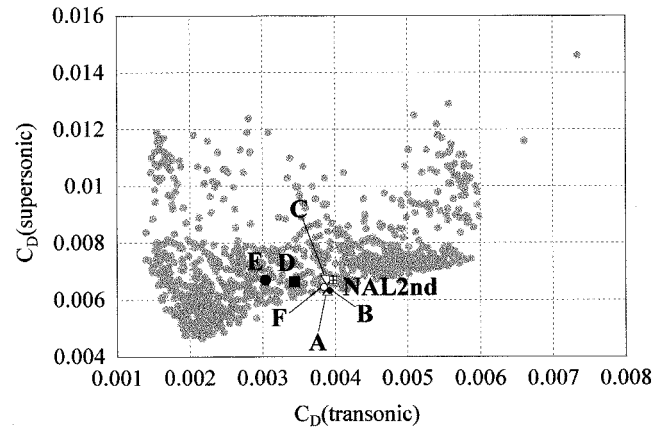

(a)

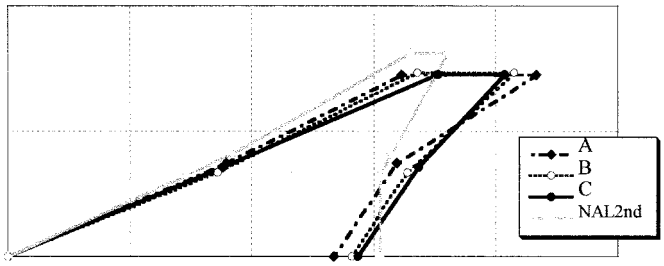

(b)

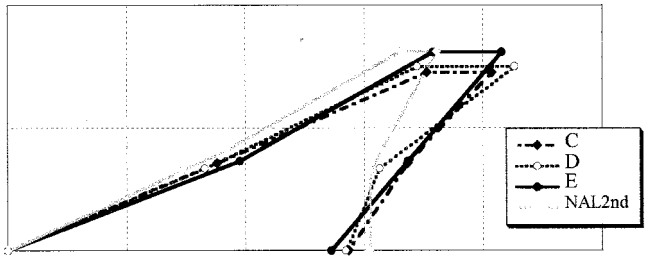

(c)

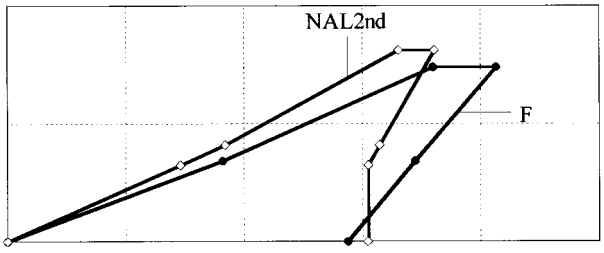

(d)

Fig. 6. Comparison of selected Pareto solutions with NAL's design. (a) NAL's design performance plotted on the projection of Pareto solutions in Fig. 7 and Pareto solutions A to F selected for comparison. (b) Planform shapes of selected Pareto solutions having similar transonic drag coefficients as NAL's design has. (c) Planform shapes of selected Pareto solutions having similar supersonic drag coefficients as NAL's design has. (d) Planform shape of Pareto solution F that performs better than NAL's design in all three objective functions.

2) Transonic drag coefficient $C_{D,t}$.
3) Bending moment at the wing root $M_{\rm root}$.

Constraints:

1) Lift coefficients $C_{L,s}$ and $C_{L,t}$ at cruise conditions.
2) Wing area.
3) Wing thickness.

TABLE II
PERFORMANCE COMPARISON AMONG SELECTED PARETO SOLUTIONS A–F AND NAL's DESIGN

	Aspect Ratio	Taper Ratio	C_D(transonic) ($\times 10^{-4}$)	C_D(supersonic) ($\times 10^{-4}$)	Bending Moment
A	1.76	0.41	38.96	62.80	18.64
B	1.79	0.28	39.25	63.32	18.19
C	1.77	0.19	38.90	66.97	17.87
D	1.89	0.29	34.38	66.52	18.89
E	2.19	0.21	30.36	67.08	19.70
F	1.82	0.19	38.43	64.61	18.17
NAL 2nd	2.20	0.10	39.73	67.00	18.31

The supersonic drag to be minimized is evaluated by using a Euler flow solver [7]. The transonic drag is evaluated by using a full potential flow solver [8]. The bending moment is evaluated by directly integrating the pressure load at the supersonic cruise condition. The flow conditions are $M_\infty = 2.0$ and $C_{L,s} = 0.1$ for supersonic cruise, and $M_\infty = 0.9$ and $C_{L,t} = 0.15$ for transonic cruise. The lift is necessary for supporting the aircraft weight at each cruise condition. The wing area is restricted for the takeoff and landing performance, and the wing thickness is restricted for the structural indignity.

The wing planform is determined by six design variables as shown in Fig. 2. The variable ranges are summarized in Table I. A wing area is fixed at $S = 60$. A chord length at the wing tip is determined automatically due to the given wing area. An airfoil shape is defined by its thickness distribution and camber line. The thickness distribution is given by a Bezier curve defined by nine polygons. The maximum thickness is constrained from 3 to 4% chord lengths. The location of the maximum thickness is also constrained from 15 to 70% chordwise locations. The thickness distributions are defined at the wing root, kink, and tip. They are linearly interpolated in the spanwise direction. The total number of polygons is 27 for the thickness definition. The camber surfaces are defined at the inboard and outboard of the wing separately. Each surface is given by the Bezier surface using four polygons in the chordwise direction and three polygons in the spanwise direction. The complete camber surface is represented by 48 polygons. Finally, the wing twist is defined by a B-spline curve with six polygons. A monotonic variation is enforced by rearranging the polygons in numerical order in the spanwise direction. In total, 66 design variables are used to control those polygons and the planform shape (note that the end polygons are fixed, except for the twist). The chromosome is therefore the string of 66 real numbers.

III. RESULTS

A. Pareto Front

MOGA is used as a design optimizer. Flow calculations were parallelized on 32 processing elements of an NEC SX-4 computer at the Computer Center of Tohoku University using the simple Master–Slave concept. The population size was set to 64, and 70 generations were run. The evolution was stopped after the progress of the Pareto front was saturated for several generations. To constrain the lift coefficient, three flow calculations

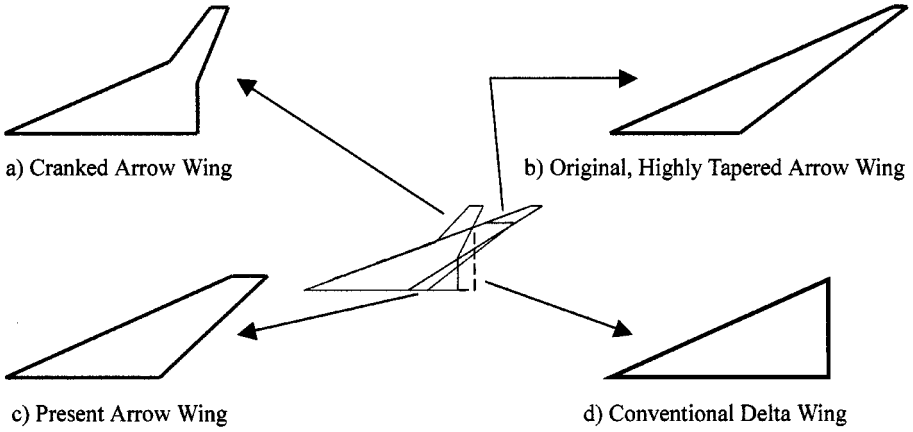

Fig. 7. Various planform shapes proposed for the supersonic wing design.

were used per drag evaluation. The total computational time was roughly 100 h.

Fig. 3 shows the resulting Pareto solutions in the three-dimensional objective function space. They form an approximate tradeoff surface. Typical planform shapes are also plotted in the figure. The extreme Pareto solutions (denoted as bending moment minimum, $C_{D,s}$ minimum, $C_{D,t}$ minimum) have physically reasonable shapes: a very short span length (corresponding to a large taper ratio as well as a low aspect ratio) for minimizing bending moment, high aspect ratios for minimizing induced drag, and larger sweep angles for minimizing wave drag. These results indicate the validity of the present optimization.

Tradeoffs between the objectives can be observed more easily in the two-dimensional projections, as shown in Figs. 4 and 5. Fig. 4 presents the tradeoffs between supersonic and transonic drag coefficients. The Pareto solutions are plotted in different symbols according to the aspect ratio. Lower drag coefficients are obtained from larger aspect ratios in general, as suggested by the standard aerodynamic theory.

In Fig. 4, the edge of the projected Pareto surface I indicates purely aerodynamic tradeoffs between supersonic and transonic flights. This curve would be the Pareto front if only these two objectives were used. However, as shown in Fig. 3, the extreme Pareto solutions for supersonic and transonic drag have too large aspect ratios, and thus they are impossible to build within a reasonable structural weight. This is true for all solutions on the edge I. The other edge of the projected Pareto surface II indicates the tradeoffs between the supersonic drag and the bending moment. (Note that the bending moment is evaluated at the supersonic flight condition.) A practical wing shape is expected to appear in this region.

Fig. 5 illustrates the tradeoffs between the bending moment and the supersonic drag. The edge of the projected Pareto surface forms a simple convex curve toward the lower left corner of the figure, representing the pure tradeoffs between these two objectives. The edge IV may be less interesting to aircraft designers because it indicates severe penalties in the drag with little improvements in the bending moment. On the other hand, edge III represents more reasonable tradeoffs. The Pareto solutions are plotted in different symbols according to the taper ratio. To be on edge III, the taper ratio of the wing should roughly be less than 0.4.

B. Comparison with the Existing Design

To evaluate the present Pareto solutions further, they are compared with the aerodynamic design of the supersonic wing for National Aerospace Laboratory's Scaled Supersonic Experimental Airplane [10]. The NAL SST Design Team has performed the following four aerodynamic designs. The first design was a selection of a planform shape among 99 different shapes by direct comparisons. The second design was performed by the warp optimization based on the linearized theory (the simplest fluid model). The third design was obtained from an inverse design to yield a natural laminar flow based on the Navier–Stokes code (the most complicated fluid model). The fourth design was then performed for a wing–fuselage configuration. Since the present optimization is based on the inviscid flow codes (the potential and Euler fluid models), NAL's second design is chosen for the comparison here. Its performance was evaluated by using the same codes in this study.

Fig. 6 and Table II summarize the comparisons of six Pareto solutions with NAL's second design. It should be noted that NAL's design appears close to edge II in Fig. 4. This indicates that edge II represents a practical solution area, as well as that the warp optimization of NAL's design has a good accuracy. Six solutions were picked up so as to represent the sensitivity of the Pareto surface. Solutions A, B, and C have transonic drag similar to NAL's design, but their supersonic drag is in the order of $A < B < C$. (Solution C and NAL's design perform alike.) To improve the supersonic performance over NAL's design, the taper ratio of the wing becomes larger, and the root chord length becomes smaller. However, there is an upper limit for the taper ratio from the observation in Fig. 5.

Solutions C, D, and E have supersonic drag similar to NAL's design and transonic drag in the order of $E < D < C$. To improve the transonic performance over NAL's design, the aspect ratio of the wing becomes larger, and the root chord length be-

comes smaller. However, the increase of the aspect ratio also results in an increase of the bending moment, as indicated in Table II.

Finally, solution F is found to outperform NAL's design in all three objectives. A common geometric feature among the three solutions A, E, and F is that their root chord lengths are shorter than the root of NAL's design. This means that they have larger taper ratios. Aerodynamic theory generally suggests an increase of the aspect ratio to improve the aerodynamic performance, as mentioned before. However, the present solutions A, E, and F all have smaller aspect ratios than NAL's design does. The resulting shape is somehow similar to the "arrow wing" planform rather than the conventional "delta wing" planform.

The arrow wing shape was originally derived from research in the late 1950's, indicating that the optimum wing planform would be a highly swept, highly tapered, arrowhead shape [11]. Attempts to incorporate such arrow wing shapes eventually failed due to design integration difficulties, aeroelastic problems, and high structural weight. Studies from the 1970's to 1980's then resulted in the "cranked arrow" wing. The cranked arrow retains the original arrow on the inboard wing only. The "cranked" forward outboard wing provides more span and a higher effective aspect ratio (Fig. 7). The main interest in the supersonic wing development has been an increase of the aspect ratio in compromise with the highly swept planform.

The present results suggest a new type of the arrow wing planform having a larger taper ratio instead of a larger aspect ratio. This means a less tapered arrow wing in contrast to the original, highly tapered arrow wing as compared in Fig. 7. In the present MOGA result, neither the cranked arrow nor the modified delta survived as a Pareto solution. The original arrow wing was abandoned due to structural problems. After 40 years of development in the structural dynamics and materials, the present arrow wing may be interesting for further studies.

ACKNOWLEDGMENT

The computational time was provided by the Computer Center, Tohoku University. The authors would like to thank National Aerospace Laboratory's SST Design Team for providing many useful data.

REFERENCES

[1] S. Wakayama and I. Kroo, "Subsonic wing planform design using multidisciplinary optimization," *J. Aircraft*, vol. 32, no. 4, pp. 746–753, 1995.

[2] C. M. Fonseca and P. J. Fleming, "Genetic algorithms for multiobjective optimization: Formulation, discussion and generalization," in *Proc. 5th Int. Conf. Genetic Algorithms*. San Mateo, CA: Morgan Kaufmann, 1993, pp. 416–423.

[3] S. Obayashi, S. Takahashi, and Y. Takeguchi, "Niching and elitist models for MOGAs," in *Parallel Problem Solving from Nature—PPSN V*. Berlin, Germany: Springer, 1998, pp. 260–269. (Lecture Notes in Computer Science).

[4] L. J. Eshelman, "The CHC adaptive search algorithm: How to have safe search when engaging in nontraditional genetic recombination," in *Foundations of Genetic Algorithms*. San Mateo, CA: Morgan Kaufmann, 1991, pp. 265–283.

[5] L. Davis, Ed., *Handbook of Genetic Algorithms*. New York: Van Nostrand, Reinhold, 1990.

[6] D. E. Goldberg, *Genetic Algorithms in Search, Optimization & Machine Learning*. Reading, MA: Addison-Wesley, 1989.

[7] J. E. Baker, "Reducing bias and inefficiency in the selection algorithm," in *Proc. 2nd Int. Conf. Genetic Algorithms*. San Mateo, CA: Morgan Kaufmann, 1987, pp. 14–21.

[8] S. Obayashi, K. Nakahashi, A. Oyama, and N. Yoshino, "Design optimization of supersonic wings using evolutionary algorithms," in *Proc. 4th ECCOMAS Computational Fluid Dynamics Conf.* Chichester, England: Wiley, 1998, pp. 575–579.

[9] A. Jameson and D. A. Caughey, "A finite volume method for transonic potential flow calculations," Amer. Instit. Aeronaut. Astronaut., Reston, VA, AIAA paper 77-677, 1977.

[10] T. Iwamiya, "NAL SST project and aerodynamic design of experimental aircraft," in *Proc. 4th ECCOMAS Computational Fluid Dynamics Conf.*, Chichester, U.K.: Wiley, 1998, vol. 2, pp. 580–585.

[11] C. P. Nelson, "Effects of wing planform on HSCT off-design aerodynamics," Amer. Inst. Aeronaut. Astronaut., Reston, VA, AIAA paper 92-2629-CP, 1992.